Uzbekov, B., Shprits, Y., Orlova, K. (2016): Scattering of Relativistic and Ultra-relativistic Electrons by Obliquely Propagating Electromagnetic Ion Cyclotron Waves. - *Journal of Atmospheric and Solar-Terrestrial Physics*, *148*, pp. 22—31.
DOI: http://doi.org/10.1016/j.jastp.2016.08.004

Scattering of Relativistic and Ultra-relativistic Electrons by Obliquely Propagating Electromagnetic Ion Cyclotron Waves

Bogdan Uzbekov[1], Yuri Y. Shprits[2,3,4], and Ksenia Orlova[1,2]

[1] - Skolkovo Institute of Science and Technology, Moscow, Russia.

[2] - Department of Earth, Planetary, and Space Sciences, University of California, Los Angeles, California, USA.

[3] - Department of Earth, Atmospheric and Planetary Sciences, Massachusetts Institute of Technology, Cambridge, Massachusetts, USA.

[4] - Helmholtz Centre Potsdam, GFZ German Research Centre For Geosciences.

Key points

1. The method presented can be applied to EMIC waves or any other wave modes;
2. First order resonance dominates the scattering of relativistic electrons up to multi-MeV energies;
3. Ion composition is a crucial parameter for quantifying scattering rates.

Electromagnetic Ion Cyclotron (EMIC) waves are transverse plasma waves that are generated in the Earth magnetosphere by ring current protons with temperature anisotropy in three different bands: below the H^+, He^+ and O^+ ion gyrofrequencies. EMIC events are enhanced during the main phase of a geomagnetic storm when intensifications in the electric field result in enhanced injections of ions and are usually confined to high-density regions just inside the plasmapause or within drainage plumes. EMIC waves are capable of scattering radiation belt electrons and thus provide an important link between the intensification of the electric field, ion populations, and radiation belt electrons. Bounce-averaged diffusion coefficients computed with the assumption of parallel wave propagation are compared to the results of the code that uses the full cold plasma dispersion relation taking into account oblique propagation of waves and higher-order resonances. We study the sensitivity of the scattering rates to a number of included higher-order resonances, wave spectral distribution parameters, wave normal angle distribution parameters, ambient plasma density, and ion composition. Inaccuracies associated with the neglect of higher-order resonances and oblique propagation of waves are compared to potential errors introduced by uncertainties in the model input parameters.

1. Introduction

1.1. Scattering by EMIC waves

Wave-particle interaction is an important aspect of radiation belt physics, and is responsible for the variability of particle fluxes observed. One type of plasma wave that is supported by the Earth's magnetosphere, and is able to effectively scatter radiation belt particles is the electromagnetic ion cyclotron (EMIC) wave [*Thorne and Kennel*, 1971; *Lyons and Thorne*, 1972]. Recent studies have suggested that EMIC waves are most efficient at scattering ultra-relativistic electrons [e.g., *Usanova et al.*, 2014; *Shprits et al.*, 2014; *Drozdov et al.*, 2015]. EMIC waves are able to cause relativistic and ultra-relativistic electron loss in a matter of hours [e.g. *Ni et al.*, 2015; *He et al.*, 2016; *Summers et al.*, 2007b; *Usanova et al.*, 2014; *Su et al.*, *2011*], and thus quantification of the effect of EMIC waves on radiation belt electrons is crucial for predicting the evolution of the radiation belt electron fluxes.

While the calculations of diffusion coefficients due to very low frequency (VLF) whistlers are done for an oblique distribution of waves [e.g., *Glauert and Horne*, 2005; *Albert*, 2005; *Shprits and Ni*, 2009; *Ni et al.*, 2008; *Gu et al.*, 2012; *Orlova and Shprits*, 2014; *Orlova et al.*, 2014], calculations of the scattering rates for EMIC waves usually assume parallel propagating waves [e.g., *Summers and Thorne*, 2003; *Summers et al.*, 2007a; *Ukhorskiy et al.*, 2010; *Usanova et al.*, 2014; *Shprits et al.*, 2014]. The likely reason is a cumbersome plasma dispersion relation and related computational difficulties required to quantify effects of oblique EMIC waves in the presence of heavy ions on the radiation belt particles. In this study, we use a semi-analytical approach described in the text below. It allows us to obtain accurate and reliable solutions for diffusion coefficients, which is challenging to obtain using a purely analytical or purely numerical approach. The method and the code developed can be used to study other plasma wave modes obliquely propagating in the presence of heavy ions and their effects on radiation belt particles with high accuracy, opening opportunities for future research. The presented method guarantees that all intersections of dispersion relation and cyclotron resonance condition curves are obtained.

Albert [2003] considered all three bands of oblique EMIC waves and investigated the sensitivity of the diffusion coefficients for EMIC waves to wave normal angle distribution and resonance numbers. He also proposed a computationally efficient technique to avoid integration over ranges of latitudes, wave normal angles and resonant numbers that are not consistent with the resonance in a prescribed wave population. Yet *Albert* [2003] made slight approximations to the exact cold plasma theory, namely a high-density approximation, which is reasonable in the case of EMIC waves, and allows for an analytical solution as a result of simpler equations. *Glauert*

and Horne [2005] have taken the results of the PADIE code calculated numerically the diffusion coefficients for the case of oblique EMIC waves, and compared them to the results of [*Summers and Thorne*, 2003], where the assumption of parallel wave propagation is made, and outlined the importance of EMIC wave obliquity. The study conducted by *Glauert and Horne* [2005], however, fixes ambient plasma density, ion composition and parameters of the wave spectral distribution. *Ni et al.* [2015] provided a useful general 14th-order polynomial equation of resonant frequencies concerning oblique EMIC wave interactions with charged particles in cold, magnetized, multi-ion plasma. The study considered multi-band EMIC waves propagating at different L-shells and having various wave normal angles. Present study fixes L-shell at $L = 4$ and only considers He band waves, but complements work of *Ni et al.* [2015] by conducting extensive sensitivity analysis of the diffusion coefficients for oblique EMIC to other model input parameters, including number of cyclotron resonances, wave spectral distribution, ambient plasma density and ion composition.

While *Albert* [2003], *Glauert and Horne* [2005] and *Summers et al.* [2007b] considered an arbitrary ratio of plasma to gyrofrequency, in the current study we use statistical models [*Carpenter and Anderson*, 1992] to calculate the ratio of plasma frequency to gyrofrequency.

In this study we focus on the He band left-hand polarized EMIC waves (L-mode), due to its typically higher amplitude and subsequent comparison to H and O bands [*Saikin et al.*, 2015]. At the same time, right-hand polarized (R-mode) EMIC waves are rarely observed experimentally [e.g. *Meredith et al.*, 2003, *Allen et al.*, 2015]. In addition, the R-mode waves are not as efficient at scattering ultra-relativistic electrons as the L-mode waves.

1.2. Code Description

We have performed calculations of the bounce-averaged diffusion coefficients for oblique EMIC waves using Full Diffusion Code (FDC) [e.g. *Ni et al.*, 2008; *Shprits and Ni*, 2009; *Gu et al.*, 2012], following the theoretical approach presented in *Glauert and Horne* [2005]. The details of the calculations are presented in the supporting information. The code is capable of computing resonant scattering rates, including first-order, Landau, and higher-order resonances and uses the methodology of *Orlova and Shprits* [2011] to integrate bounce period and momentum diffusion coefficients, avoiding uncertainty at the mirror point.

Substituting resonance conditions for wave-particle interactions into the cold plasma dispersion relation yields a fourteenth order polynomial with respect to the wave frequency ω. For the version of the code developed for this study, the coefficients are derived semi-analytically using the Matlab Symbolic Toolbox and then incorporated into the code explicitly. Coefficients of the

polynomial are not presented in this work, as they are very cumbersome. The roots of the polynomial, satisfying both cold plasma dispersion relation and resonance conditions, are computed using a standard polynomial root finder. Only roots that lie between the lower and upper cut-off frequencies of the wave are considered. The roots are then checked on their R-mode or L-mode origin, and filtered according to the mode under consideration (e.g. R-mode roots are not considered, when studying the effects of the L-mode waves only). The dispersion relation derivative, $(\partial\omega/\partial k)|_{\mathcal{D}=0}$, which is required to compute local diffusion coefficients, is also calculated semi-analytically with the help of the Matlab Symbolic Toolbox. The resulting derivative formula is very cumbersome and therefore not presented here.

From the mathematical standpoint, the dispersion relation derivative $(\partial\omega/\partial k)|_{\mathcal{D}=0}$, as well as coefficients of the polynomial derived substituting resonance conditions into the dispersion relation $\mathcal{D}(k,\omega,X)=0$, are functions of local magnetic field value, ambient plasma density n_e, plasma ion composition (parameters $\zeta_{H^+}=n_{H^+}/n_e$, $\zeta_{He^+}=n_{He^+}/n_e$, and $\zeta_{O^+}==n_{O^+}/n_e$), particle energy, local pitch angle α, wave normal angle θ and resonant number n. The choice of these variables makes the code relatively easy to adapt to studies of other plasma wave modes and their effects on the trapped radiation at various magnetospheres.

We assume distributions of wave normal angle $g(\theta)$ and wave spectral density $B^2(\omega)$ to be Gaussian:

$$B^2(\omega)=\begin{cases}A^2 exp\left(-\left(\dfrac{\omega-\omega_m}{\delta\omega}\right)^2\right), & \omega_{lc}\le\omega\le\omega_{uc}\\ 0, & otherwise\end{cases}$$

where ω_m and $\delta\omega$ are distribution maximum and bandwidth respectively, ω_{lc} and ω_{uc} are lower and upper cut-off frequencies, and A is a normalisation factor. And for the wave angular spread:

$$g(X)=\begin{cases}exp\left(-\left(\dfrac{X-X_m}{X_w}\right)^2\right), & X_{min}\le X\le X_{max}\\ 0, & otherwise\end{cases}$$

where $X=tan(\theta)$, X_w is the angular distribution bandwidth, X_m is the peak value, and X_{min} and X_{max} are the cut-off values.

We set MLT presence of the waves to 100%. In order to obtain more realistic scattering rates, our diffusion coefficients need to be scaled by the width of the MLT sector where waves are present. The scaling is performed by simple multiplication of the coefficients by realistic MLT presence. Maximum latitude of the wave propagation is set to 20° following statistical study of *Meredith et al.* [2003].

We have validated the code by comparing our results with those from *Glauert and Horne* [2005].

2. Sensitivity Simulations

In this section, we first study contribution of the Landau, first-order and higher-order resonances to the bounce-averaged pitch angle diffusion coefficients for oblique EMIC waves. This analysis allows us to estimate the number of resonances that needs to be included into calculations to give sufficiently accurate results. We then move to comparison of the scattering rates calculated for EMIC waves propagating parallel to the magnetic field and for the case of oblique propagation of waves. Finally, we study sensitivity of the diffusion coefficients for oblique EMIC waves to the key model input parameters – wave spectral distribution, wave normal angle distribution, ambient plasma density, and ion composition.

2.1 Contribution of Various Resonances

Figure 1 shows the contribution of various resonances to the bounce-averaged pitch angle diffusion coefficients for electron energies of 3, 5, 7, and 10 MeV. The scattering rates were computed at $L = 4$ with the input parameters summarized in Table 1.

Table 1. Model input parameters used to obtain the results shown in Figure 1 and Figure 2

Parameters	*Values*
Wave normal angle distribution	$\theta_{lc} = 0°, \theta_{uc} = 75°, \theta_m = 30°, \delta\theta = 30°$
Wave spectral distribution	$\omega_{lc} = 2.5\Omega_{O^+}, \omega_{uc} = 3.5\Omega_{O^+}, \omega_m = 3\Omega_{O^+},\ \delta\omega = 0.5\Omega_{O^+}$ [*Summers et al.*, 2007b]
Wave amplitude	$dB = 1\ nT$
Plasma density model	*Carpenter and Anderson* [1992]
Ion composition	$\zeta_{H^+} = 0.7n_e, \zeta_{He^+} = 0.2n_e, \zeta_{O^+} = 0.1n_e$ [*Meredith et al.*, 2003]
Resonant numbers	$n = -5, \dots, 0, \dots, 5$

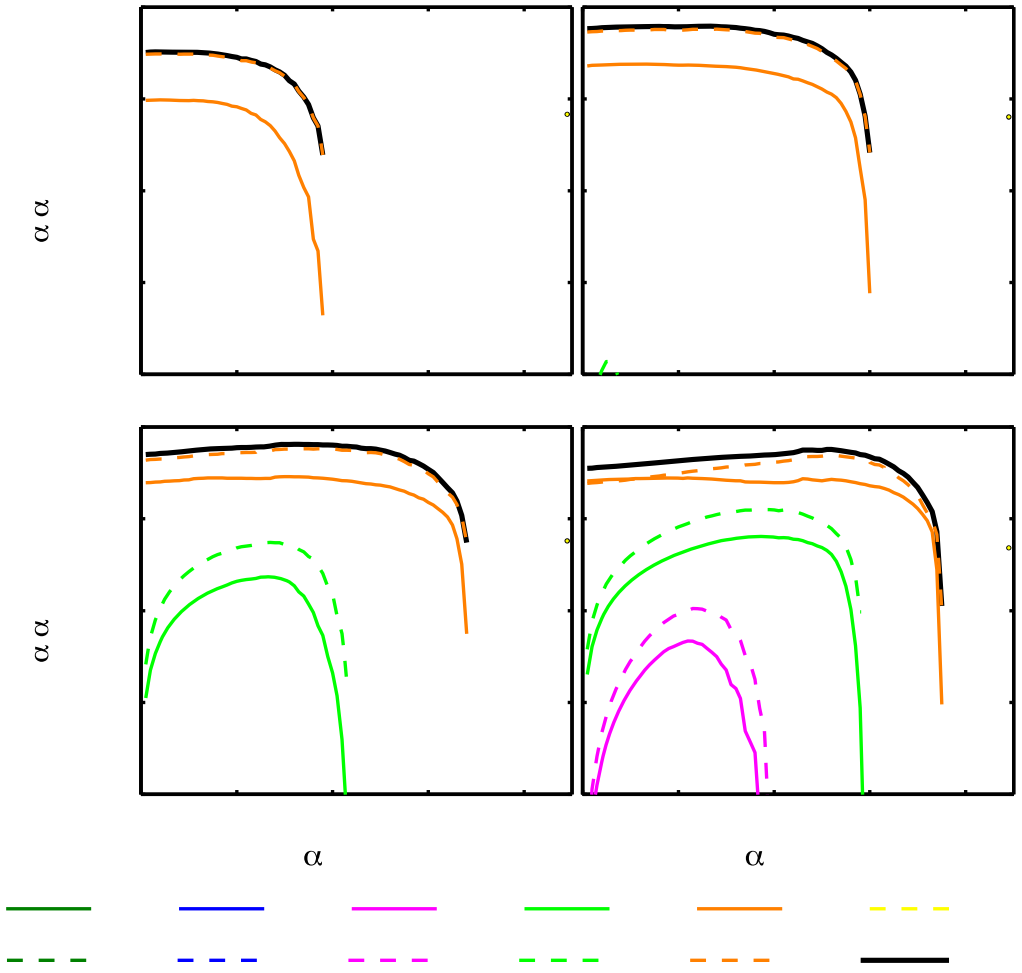

Figure 1. Contribution of various resonances into the bounce-averaged pitch angle diffusion coefficients for oblique EMIC waves at L=4 for energies of a) 3 MeV, b) 5 MeV, c) 7 MeV and d) 10 MeV, respectively.

From Figure 1 we see that the principal resonance ($n = 1$) can give a fairly good estimate of the diffusion coefficients at energies of up to 7 MeV, while at $E = 10$ MeV, the resonance represented by $n = -1$ number overtakes the principal resonance at pitch angles below 20°, which should be taken into account. It is interesting to note resonances appearing in pairs corresponding to $|n|$, and how the range of electrons' pitch angles affected by diffusion is decreasing with growing $|n|$.

Another interesting observation is the absence of $n = 0$ (Landau) resonance in Figure 1. Zeroth resonance has appeared, however, in the case of four-fold increase in the plasma density value (not shown in this paper). Nevertheless, the contribution of Landau resonance was at least several orders of magnitude smaller compared to contributions from cyclotron resonances in all of our simulations. Finally we notice that more resonances contribute to the scattering rates with energy growing.

2.2 Comparison with the Case of Parallel Wave Propagation

We continue by comparing the diffusion coefficients calculated for oblique EMIC waves and for the case of field-aligned propagation. We illustrate the results of the simulations in Figure 2, and present model input parameters that were used in Table 1. We have treated the case of field-aligned waves using the theoretical approach from *Summers et al.* [2007a], taking into account factor of two discrepancy reported by *Albert* [2007].

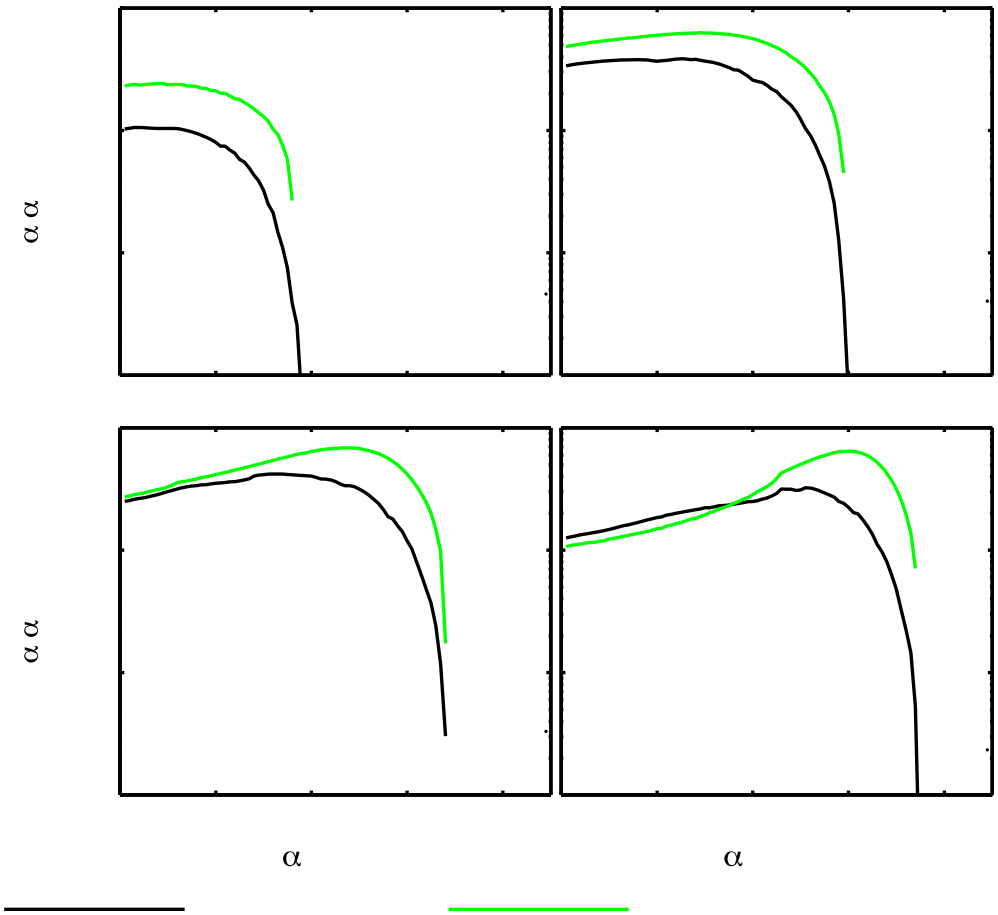

Figure 2. Comparison of bounce-averaged pitch angle diffusion coefficients calculated for oblique EMIC waves and for the case of field-aligned wave propagation at L=4. Panels correspond to energies of a) 3 MeV, b) 5 MeV, c) 7 MeV and d) 10 MeV.

We find that obliquity of EMIC waves leads to an overall decrease of their ability to scatter ultra-relativistic outer radiation belt electrons, when compared to field-aligned waves. Importantly, we can also see that obliquity of EMIC waves does not change the range of equatorial pitch angles that can be affected by electron scattering. Both implications are further confirmed below, when looking at a sensitivity of electron scattering rates by EMIC waves to the wave normal angle distribution.

2.3 Sensitivity of the Scattering Rates to Changes in the Wave and Plasma Properties

We start sensitivity studies of the diffusion coefficients for EMIC waves by varying the wave spectral distribution parameters. The inputs used are summarized in Table 2, and the results are comprised in Figure 3. We used three different sets of parameters of the wave spectral distribution: the first is adopted from *Summers et al.* [2007b], the second set is from *Usanova et al.* [2014], and finally, the third set of spectral distribution parameters is the same as the latter, but with the higher upper cutoff frequency, which is the same as used in *Li et al.* [2007].

Table 2. Model input parameters used to study sensitivity of the diffusion coefficients to the parameters of the wave spectral distribution

Parameters	*Values*
Wave normal angle distribution	$\theta_{lc} = 0°, \theta_{uc} = 75°, \theta_m = 30°, \delta\theta = 30°$
Wave spectral distribution	Set 1 [*Summers et al.*, 2007b]: $\omega_{lc} = 2.5\Omega_{O^+}, \omega_{uc} = 3.5\Omega_{O^+}, \omega_m = 3\Omega_{O^+}, \delta\omega = 0.5\Omega_{O^+}$ Set 2 [*Usanova et al.*, 2014]: $\omega_{lc} = 2.16\ \Omega_{O^+}$, $\omega_{uc} = 3.84\Omega_{O^+}, \omega_m = 2.96\Omega_{O^+}, \delta\omega = 0.4\Omega_{O^+}$ Set 3: $\omega_{lc} = 2.16\ \Omega_{O^+}$, $\omega_{uc} = 3.95\ \Omega_{O^+}$, $\omega_m = 2.96\Omega_{O^+}, \delta\omega = 0.4\Omega_{O^+}$
Wave amplitude	$dB = 1\ nT$
Plasma density model	[*Carpenter and Anderson*, 1992]
Ion composition	$\zeta_{H^+} = 0.7n_e, \zeta_{He^+} = 0.2n_e, \zeta_{O^+} = 0.1n_e$ [*Meredith et al.*, 2003]
Resonant numbers	$n = -5, \dots, 0, \dots, 5$

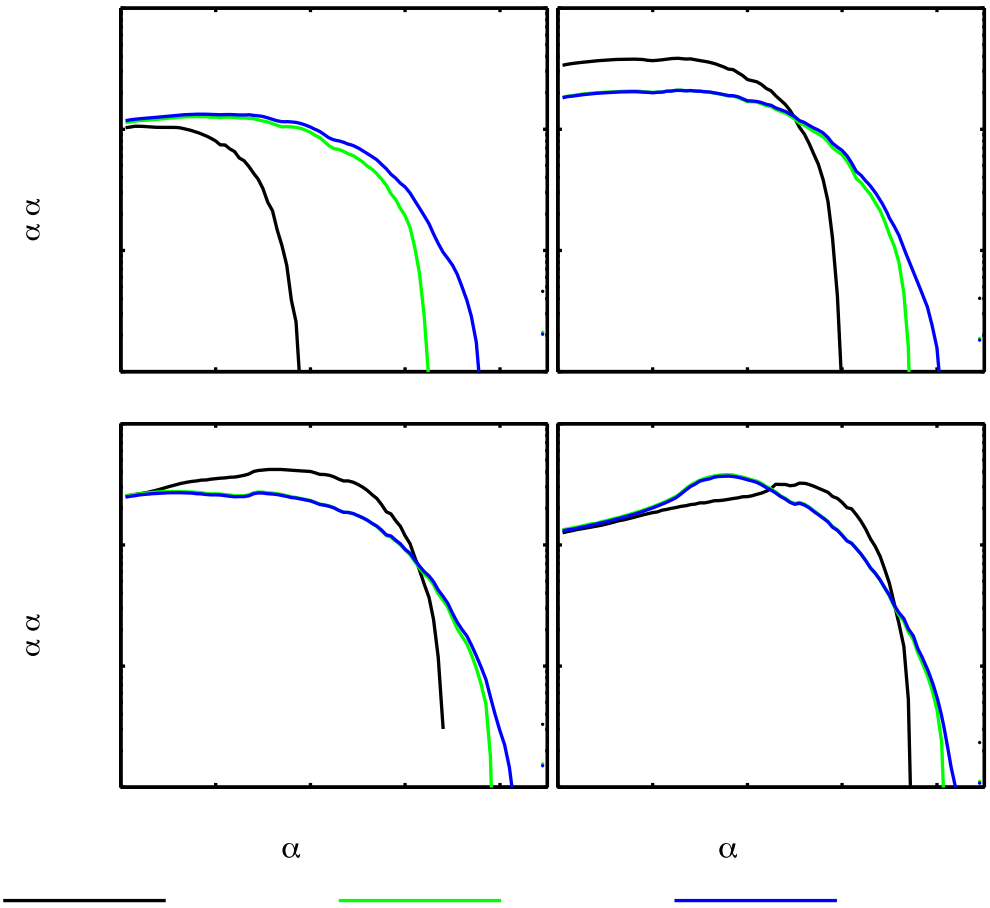

Figure 3. Sensitivity of the bounce-averaged pitch angle diffusion coefficients for oblique EMIC waves at L=4 to the parameters of the wave spectral distribution. Black, green and blue lines denote results obtained using input parameters of set 1, set 2, and set 3, respectively, from Table 2. Panels correspond to energies of a) 3 MeV, b) 5 MeV, c) 7 MeV and d) 10 MeV.

Changes in the parameters of the wave spectral distributions lead to changes in the range of electrons' equatorial pitch angles that can be affected by EMIC waves through diffusion. We note that electron scattering rates appear to be more sensitive to the parameters of wave spectral distribution at lower energies. For lower energy wave distribution changes the range of pitch angles for which waves can resonate with electrons, while for higher energies for a broader range of electron pitch angles, resonance conditions are satisfied and wave parameters play less of a role. Indeed, the greatest sensitivity is observed at energy of 3 MeV, where we see a shift of the maximum equatorial pitch angle of electrons to be scattered into the loss cone by about 30 and 40 degrees for the input parameters of set 2 and set 3 respectively. Finally, high sensitivity of electron scattering rates due to interaction with EMIC waves to the upper cutoff frequency is to be emphasized. We can see it by comparing scattering rate curves in Figure 3 corresponding to sets 2 and 3. The effect was previously confirmed by studies of field-aligned EMIC waves, e.g. *Li et al.* [2007].

We continue the sensitivity studies by varying parameters of the wave normal angle distribution. We give model input parameters that were used in Table 3 and demonstrate the results of simulations in Figure 4.

Table 3. Model input parameters used to study sensitivity of the diffusion coefficients to the parameters of the wave normal angle distribution (corresponding results are shown in Figure 4)

Parameters	*Values*
Wave normal angle distribution	Set 1: $\theta_{lc} = 0°, \theta_{uc} = 75°, \theta_m = 30°, \delta\theta = 30°$ Set 2: $\theta_{lc} = 0°, \theta_{uc} = 75°, \theta_m = 30°, \delta\theta = 10°$ Set 3: $\theta_{lc} = 0°, \theta_{uc} = 75°, \theta_m = 15°, \delta\theta = 30°$
Wave spectral distribution	$\omega_{lc} = 2.5\Omega_{O^+}, \omega_{uc} = 3.5\Omega_{O^+}, \omega_m = 3\Omega_{O^+}, \delta\omega = 0.5\Omega_{O^+}$ [*Summers et al.*, 2007b]
Wave amplitude	$dB = 1\ nT$
Plasma density model	*Carpenter and Anderson* [1992]
Ion composition	$\zeta_{H^+} = 0.7n_e, \zeta_{He^+} = 0.2n_e, \zeta_{O^+} = 0.1n_e$ [*Meredith et al.*, 2003]
Resonant numbers	$n = -5, \dots, 0, \dots, 5$

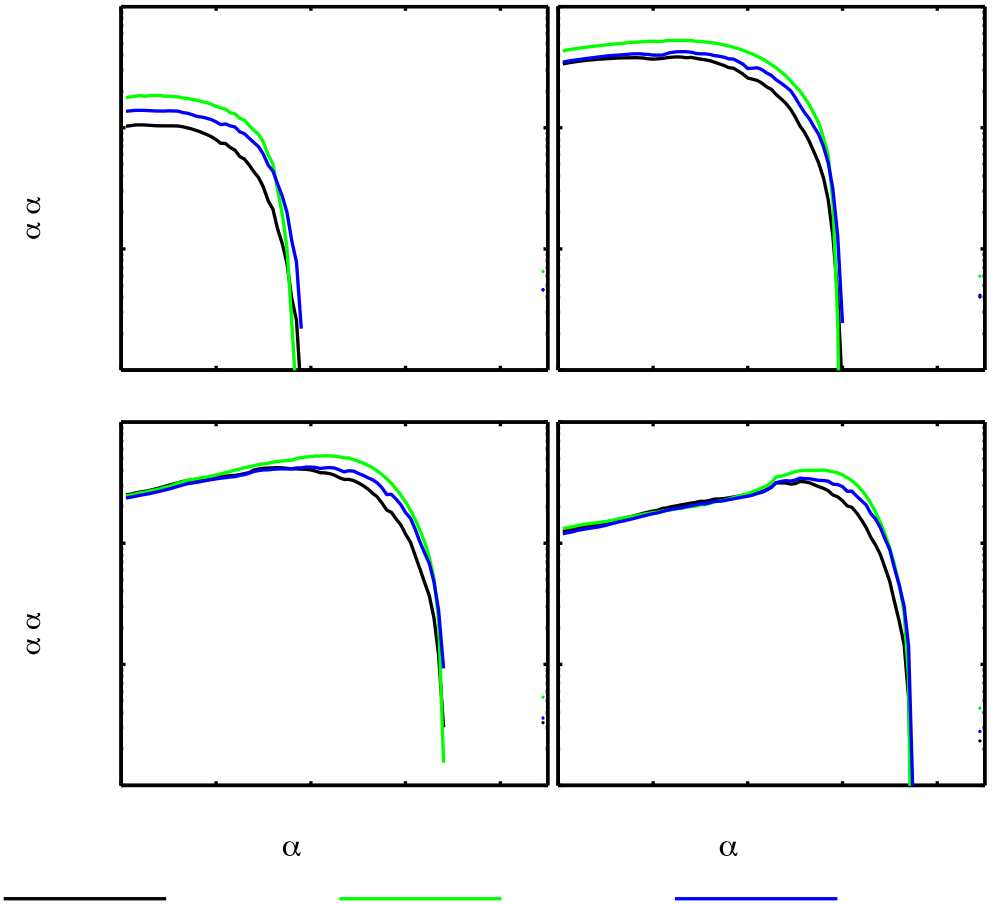

211

212 ***Figure 4. Sensitivity of the bounce-averaged pitch angle diffusion coefficients for oblique EMIC waves at L=4 to***
213 ***the parameters of the wave normal angle distribution. Black, green and blue lines denote results obtained using***
214 ***input parameters of set 1, set 2 and set 3 respectively from Table 3. Panels correspond to energies of a) 3 MeV, b)***
215 ***5 MeV, c) 7 MeV and d) 10 MeV.***

216 From Figure 4 we confirm a conclusion drawn from Figure 2 above, namely that changing
217 obliquity of EMIC waves does not lead to substantial changes in the range of equatorial pitch
218 angles to be affected by diffusion, unless waves turn out to be more oblique than assumed in this
219 study. At each panel of Figure 4, we see that all the plots corresponding to various wave normal
220 angle distributions terminate at almost exactly the same value of the equatorial pitch angle.

We move on to analysis of sensitivity of the diffusion coefficients for oblique EMIC waves to ambient plasma density. Input parameters that were used in the study are depicted in Table 4. The reference plasma density corresponds to statistical model of *Carpenter and Anderson* [1992] at $L = 4$. Plasma density is then increased by a factor of two and four, which approximately corresponds to three and six standard deviations, respectively, of the statistical plasmasphere density model by *Sheeley et al.* [2001]. The results of the study are shown in Figure 5.

Table 4. Model input parameters used to study sensitivity of the diffusion coefficients to plasma density.

Parameters	*Values*
Wave normal angle distribution	$\theta_{lc} = 0°, \theta_{uc} = 75°, \theta_m = 30°, \delta\theta = 30°$
Wave spectral distribution	$\omega_{lc} = 2.5\Omega_{O^+}, \omega_{uc} = 3.5\Omega_{O^+}, \omega_m = 3\Omega_{O^+}, \delta\omega = 0.5\Omega_{O^+}$ [*Summers et al.*, 2007b]
Wave amplitude	$dB = 1\ nT$
Plasma density model	Case 1: n_e according to *Carpenter and Anderson* [1992] Case 2: $2n_e$ Case 3: $4n_e$
Ion composition	$\zeta_{H^+} = 0.7n_e, \zeta_{He^+} = 0.2n_e, \zeta_{O^+} = 0.1n_e$ [*Meredith et al.*, 2003]
Resonant numbers	$n = -5, \dots, 0, \dots, 5$

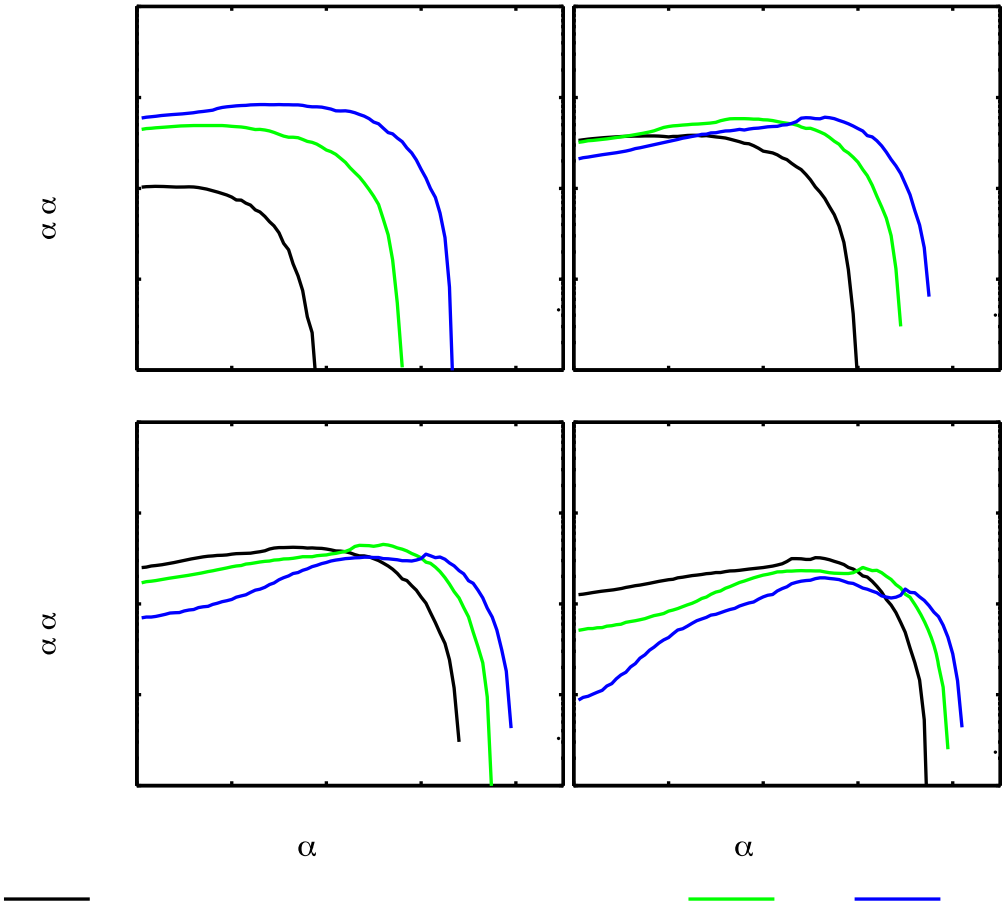

Figure 5. Sensitivity of the bounce-averaged pitch angle diffusion coefficients for oblique EMIC waves at L=4 to plasma density. Black, green and blue lines represent the case of plasma density n_e corresponding to Carpenter and Anderson [1992], and cases of two-time and four-time increase of n_e respectively. Panels correspond to energies of a) 3 MeV, b) 5 MeV, c) 7 MeV and d) 10 MeV.

From Figure 5 we note high sensitivity of the diffusion coefficients to plasma density – much higher, when compared to sensitivity to the parameters of wave normal angle distribution. We see that at all energies, growing plasma density leads to an increase of the range of equatorial pitch angles of electrons to be scattered by EMIC waves.

Significantly, ignoring the increasing range of electron equatorial pitch angles to be deflected by EMIC waves, we observe two opposite effects of increasing plasma density at electron energies of 3 MeV and 10 MeV. We note a dramatic enhancement in the ability of EMIC waves to scatter 3 MeV electrons with increasing plasma density, while at the same time a remarkable weakening of their effect on 10 MeV electrons, with panels b) and c) of Figure 5 corresponding to a transition between the two modes.

Finally, we conduct a sensitivity analysis of the diffusion coefficients for oblique EMIC waves to ion composition. We use four different sets of ion number densities: given by *Meredith et al.* [2003], *Horwitz et al.* [1984], and also simply $\boldsymbol{H^+}$ plasma and plasma containing only 2% of each $\boldsymbol{He^+}$ and $\boldsymbol{O^+}$ ions. All the input parameters used in the simulation are summarized in ***Table 5***, and the results are presented in ***Figure 6***.

Table 5. Model input parameters used to study sensitivity of the diffusion coefficients to ion composition

Parameters	*Values*
Wave normal angle distribution	$\theta_{lc} = 0°, \theta_{uc} = 75°, \theta_m = 30°, \delta\theta = 30°$
Wave spectral distribution	$\omega_{lc} = 2.5\Omega_{O^+}, \omega_{uc} = 3.5\Omega_{O^+}, \omega_m = 3\Omega_{O^+}, \ \delta\omega = 0.5\Omega_{O^+}$ [*Summers et al.*, 2007b]
Wave amplitude	$dB = 1\ nT$
Plasma density model	*Carpenter and Anderson* [1992]
Ion composition	Set 1 [*Meredith et al.*, 2003]: $\zeta_{H^+} = 0.7n_e, \zeta_{He^+} = 0.2n_e, \zeta_{O^+} = 0.1n_e$ Set 2: $\zeta_{H^+} = 0.96n_e, \zeta_{He^+} = 0.02n_e, \zeta_{O^+} = 0.02n_e$ Set 3: $\zeta_{H^+} = n_e, \zeta_{He^+} = 0, \zeta_{O^+} = 0$ Set 4 [*Horwitz et al.*, 1984]: $\zeta_{H^+} = 0.6n_e, \zeta_{He^+} = 0.37n_e, \zeta_{O^+} = 0.03n_e$
Resonant numbers	$n = -5, \dots, 0, \dots, 5$

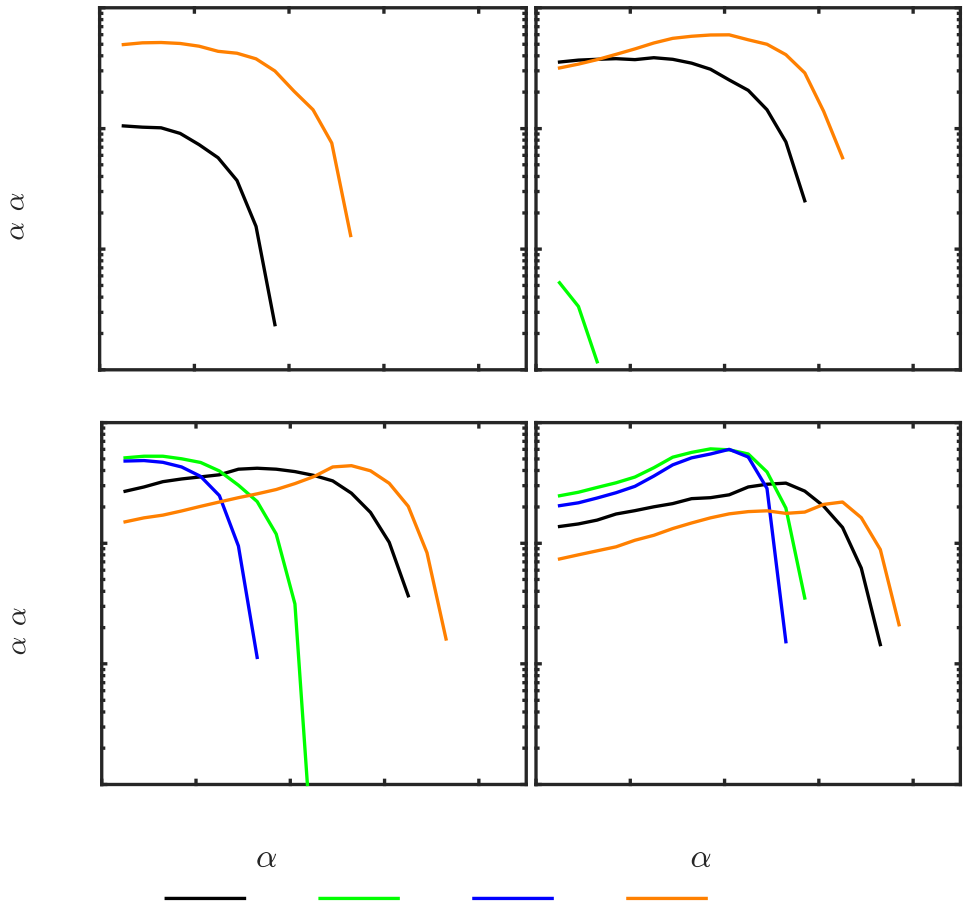

Figure 6. Sensitivity of the bounce-averaged pitch angle diffusion coefficients for oblique EMIC waves at L=4 to ion composition. Black, green, blue and orange lines denote results obtained using input parameters of set 1, set 2, set 3 and set 4 respectively from Table 5.

Figure 6 suggests that ion composition, which is very much unknown during storms [e.g. *Moldwin*, 1997; *Kistler and Mouikis*, 2015], appears to be a key factor determining the lowest energy that can be scattered by EMIC waves. Comparing the curves for sets 2 and 3, one can also notice that the addition of even a small number of heavy ions leads to notable changes in scattering by EMIC waves, as mentioned by *Albert* [2003]. Importantly, both scattering timescales associated with EMIC waves and the range of electrons' pitch angles affected are altered significantly by varying ion composition.

Given great variability of the ion composition in the plasmasphere during storm time [e.g. *Kistler and Mouikis*, 2015; *Gallagher et al.*, 2000] and high sensitivity (compared to wave spectral and wave normal angle distributions and ambient plasma density) of electron scattering by EMIC on the composition, we conclude that it is the key ingredient necessary for a good agreement of theoretical models with in-situ observations of radiation belt electrons lifetimes.

3. Discussion

3.1 Contribution of various resonances

By studying the contribution of various cyclotron resonance numbers into an overall diffusion coefficient associated with EMIC waves, we showed that for a wide range of energies (from 3 MeV to 10 MeV in our work) and given a realistic ambient plasma density, it is reasonable to neglect higher order resonances, as well as Landau resonances, when studying oblique EMIC waves. This does not mean obliquity should be ignored, because the wave normal angle is still a part of the resonance condition and dispersion relation equations, and therefore affects scattering rates (see Figure 2). We observed a growing contribution of higher-order resonances with increasing electron energies. Scattering rates associated with those resonances are still orders of magnitude smaller than the rates provided by $|n| = 1$ resonances.

3.2 Sensitivity analysis

Wave spectral distribution

We studied the sensitivity of the diffusion coefficients by adopting wave spectral distributions from *Summers et al.* [2007b] and *Usanova et al.* [2014] and assuming the wave normal angle of $\theta_m = 30^{\circ}$. We showed that changing the spectral distribution leads to a dramatic alteration of the range of electron equatorial pitch angles being affected by oblique EMIC waves. For the energy of 3 MeV, the changes accounted for $30° - 40°$. We confirmed high sensitivity of the diffusion coefficients for oblique EMIC to the upper cutoff frequency reported in *Li et al.* [2007] for the case of field-aligned waves.

Wave normal angle distribution

Even though obliquity of EMIC waves changes scattering rates of ultra-relativistic electrons in comparison with field aligned waves, we have not noted significant changes in scattering rates when varying the maximum of wave normal angle distribution from $\theta_m = 30^{\circ}$ to $\theta_m = 15^{\circ}$, and varying the distribution bandwidth from $\delta\theta = 30°$ to $\delta\theta = 10°$. Neither the value of the diffusion coefficients, nor the range of equatorial pitch angles of electrons scattered by the prescribed wave population were changing appreciably. It is important to note that these observations are valid unless waves turn out to be more oblique, say $\theta_m = 60^{\circ}$ or $\theta_m = 80^{\circ}$, which has been observed for selected storms in the recent statistical studies [e.g. *Saikin et al.*, 2015; *Allen et al.*, 2015].

Plasma density

Adopting the values of ambient plasma density prescribed by *Carpenter and Anderson* [1992] at $L = 4$, and increasing the density by three and by six standard deviations defined by the model of *Sheeley et al.* [2001], we demonstrated high sensitivity of the scattering rates to this

parameter. For instance, one can notice one-two orders of magnitude changes in the value of the diffusion coefficients when changing the value of plasma density in Figure 5, as well as changes of affected pitch angles by $20° - 30°$ at electron energies of 3 MeV and $5° - 10°$ for the energy of 10 MeV. In our simulation, increasing ambient plasma density always leads to an increase in electron pitch angles that are able to resonantly interact with EMIC waves. As for the scattering rates, we observed its one-two orders of magnitude increase for electron energy of 3 MeV and its significant decrease for electron energies of 10 MeV, especially at the lower pitch angles.

Ion composition

In order to investigate sensitivity of electron scattering rates caused by EMIC waves, we used four different sets of parameters. Two were adopted from *Meredith et al.* [2003] and from *Horwitz et al.* [1984]. The other two represented pure hydrogen plasma and plasma mainly consisting of hydrogen ions, but for 2% additional amount of each helium and oxygen ions. It was shown that the addition of even a small number of heavy ions leads to notable changes in diffusion coefficients. Both scattering rates and the range of pitch angles are affected. Furthermore, given high variability of the ion composition during magnetic storms, we conclude that ion composition is a key factor determining the minimum electron energy to interact with EMIC waves, as well as scattering rates of ultra-relativistic electrons caused by EMIC waves.

3.3 General remarks

We should emphasize that conclusions of our work are based on the assumption that waves are quasi-parallel, e.g. $\theta_m = 30^{\circ}$. If waves turn out to be more oblique than in this study, higher order resonances may play a more important role. Future detailed statistical analysis of the wave measurements will be required to validate this assumption. Additionally, we focused on the case of left-hand polarized He band waves. The choice is based on the statistical study of *Saikin et al.* [2015], who showed that He band waves statistically have a higher overall occurrence rate, as well as higher amplitudes, when compared to H and O EMIC bands.

Notably, the results obtained in the study possess the accuracy of an analytical solution as a result of using the full cold plasma dispersion relation. Thus, presented research can be used as a benchmark for future validation of various numerical methods.

With regards to the assumption of cold plasma, *Silin et al.* [2011] and *Chen et al.* [2011], [2013] showed that assumption of cold plasma theory may lead to significant errors when quantifying the effects of EMIC waves on radiation belt relativistic and ultra-relativistic electrons. Non-resonant and non-linear interactions may also contribute to electron scattering. It was shown in the past that for EMIC waves with amplitude of several nT nonlinear effects such as phase bunching and phase trapping may play important role and cause significant deviations form the

results of quasi-linear model [e.g. *Albert and Bortnik*, 2009; *Su et al.*, 2012; 2013]. Thus, the assumption of non-thermal motion of plasma particles, as well as quasi-linear approach, has to be challenged in our future studies.

It is interesting to notice that EMIC waves can violate the second adiabatic invariant of nearly equatorially mirroring electrons and provide pitch-angle scattering for a wide range of electron energies and L-shells inside and outside the plasmasphere [*Shprits*, 2009]. Another potential mechanism for scattering equatorially mirroring electrons is bounce resonance by fast magnetosonic waves [*Shprits*, 2016].

In the future we are planning to use the new diffusion coefficients for oblique EMIC waves with one of the radiation belt codes that computes particle phase space densities and fluxes – Versatile Electron Radiation Belt code [e.g. *Shprits et al.*, 2008]. This study would help to further quantify the effect of oblique EMIC waves on the radiation belt particle fluxes, which is of utmost interest from the perspective of space weather applications.

4. Summary and Conclusions

We have studied pitch angle scattering of ultra-relativistic electrons by obliquely propagating EMIC waves in the Earth's outer radiation belt. Note that the conclusion below corresponds to the most frequently observed He band and may or may not be valid for other bands. The investigation of other EMIC wave bands will be a subject of future studies. We used a full cold plasma dispersion relation that was derived semi-analytically using Matlab Symbolic Toolbox, and improved Full Diffusion Code (FDC) to calculate bounce-averaged pitch angle diffusion coefficients for oblique EMIC waves.

We compared bounce-averaged diffusion coefficients computed with the assumption of parallel wave propagation to the results of our code that uses the full cold plasma dispersion relation, taking into account the oblique propagation of waves and higher-order resonances. We have quantified the sensitivity of ultra-relativistic electron pitch angle scattering rates by EMIC waves to the model input parameters – wave spectral distribution, wave normal angle distribution, ambient plasma density and ion composition.

The main conclusions of the work are as follows:

1. From the results of studying contribution of various resonances, we demonstrate that in our simulations for energies up to approximately 7 MeV, the primary resonance ($n = 1$) plays a dominant role. For higher energies, both $n = \pm 1$ resonances should be taken into account. For the presented simulations, other resonances, including Landau resonance, can be neglected.

2. Sensitivity analysis conducted in this work leads us to the following conclusions:

- Obliquity of EMIC waves leads to an overall decrease of ability of EMIC waves to scatter ultra-relativistic electrons;
- Obliquity of EMIC waves does not substantially change the range of equatorial pitch angles of electrons that are able to resonate with EMIC waves, unless the waves turn out to be much more oblique than assumed in this study;
- Electrons of higher values of equatorial pitch angles can resonate with EMIC waves when the plasma density is higher and there is a substantial wave power close to the local ion gyrofrequency;
- Increases in background plasma density cause enhancement of electron scattering by EMIC waves at energies of approximately (3-5 MeV), and weakening at higher energies (7-10 MeV);
- Diffusion coefficients for oblique EMIC waves appear to be most sensitive to the assumed ion composition. The sensitivity to realistic variations of wave spectral distribution, wave normal angle distribution, and ambient plasma density show that these factors can also determine scattering rates but to a lesser degree;
- The lowest electron energy to be scattered by EMIC waves is most sensitive to ion composition of ambient plasma;
- Uncertainty in the model input parameters and neglect of oblique wave propagation lead to comparable errors in diffusion coefficients for EMIC waves (yet uncertainty in ion composition leads to greater errors).

3. The approach used in this work and the improved Full Diffusion Code (FDC) for oblique EMIC waves enables studies of other plasma waves affecting magnetically trapped radiation in magnetic fields of Earth and outer planets.

4. The presented method can be used to quantify scattering rates by other wave modes that depend on the ion composition. The results obtained with the presented method can serve as a benchmark for future validation of various approximate numerical methods.

Acknowledgments

We would like to thank Lynn Kistler, Matina Gkioulidou, Maria Usanova, Adam Kellerman and Alexander Drozdov for their contribution and advice. Support at UCLA was provided by NASA grant NNX10AK99G, NNX13AE34G, NSF grant 443869-YS-21686, and UC Lab Fee grant #116720, Horizon 2020 #637302. We would like to thank International Space Science Institute (Bern) for the support provided.

All data for this paper are properly cited and referred to in the reference list.

References

Albert, J. M. (2003) Evaluation of quasi-linear diffusion coefficients for EMIC waves in a multispecies plasma, *J. Geophys. Res. Space Physics*, 108, A6, ISSN 2156-2202, http://dx.doi.org/10.1029/2002JA009792.

Albert, J. M. (2007), Simple approximations of quasi-linear diffusion coefficients, *J. Geophys. Res.*, 112, A12202, doi:10.1029/2007JA012551.

Albert, J. M., and J. Bortnik (2009a), Nonlinear interaction of radiation belt electrons with electromagnetic ion cyclotron waves, *Geophys. Res. Lett.*, 36, L12110, doi:10.1029/2009GL038904.

Allen, R. C., J.-C. Zhang, L. M. Kistler, H. E. Spence, R.-L. Lin, B. Klecker, M. W. Dunlop, M. André, andV. K. Jordanova (2015), A statistical study of EMIC waves observed by Cluster: 1. Wave properties, *J. Geophys. Res. Space Physics*, 120, 5574–5592, doi:10.1002/ 2015JA021333.

Carpenter, D. L., R.R. Anderson, (1992) An ISEE/Whistler model of equatorial electron density in the magnetosphere, *J. Geophys. Res. Space Physics*, 97, A2, 1097-1108, ISSN 2156-2202, http://dx.doi.org/10.1029/91JA01548.

Chen, L., R. M. Thorne, and J. Bortnik (2011), The controlling effect of ion temperature on EMIC wave excitation and scattering, *Geophys. Res. Lett.*, 38, L16109, doi:10.1029/2011GL048653.

Chen, L., R. M. Thorne, Y. Shprits, and B. Ni (2013), An improved dispersion relation for parallel propagating electromagnetic waves in warm plasmas: Application to electron scattering, *J. Geophys. Res. Space Physics*, *118*, 2185–2195, doi:10.1002/jgra.50260.

Gallagher, D. L., Craven, P. D., Comfort, R. H. (2000), Global core plasma model, *J. Geophys. Res. Space Physics*, 105, A8, 18819-18833 ISSN 2156-2202, doi: 10.1029/1999JA000241.

Glauert, S. A., and R. B. Horne (2005), Calculation of pitch angle and energy diffusion coefficients with the PADIE code, *J. Geophys. Res.*, 110, A04206, doi:10.1029/2004JA010851.

Gu, X., Y. Y. Shprits, and B. Ni (2012), Parameterized lifetime of radiation belt electrons interacting with lower-band and upper-band oblique chorus waves, *Geophys. Res. Lett.*, 39, L15102, doi:10.1029/2012GL052519.

He, F., et al. (2016), Combined scattering loss of radiation belt relativistic electrons by simultaneous three-band EMIC waves: A case study, *J. Geophys. Res. Space Physics*, 121, 2169-9402, doi:10.1002/2016JA022483.

Kistler L.M. AND C.G. Mouiskis (2015), The Inner Magnetosphere Ion Composition and Local Time Distribution over a Solar Cycle, submitted to *J. Geophys. Res.*

Li, W., Shprits, Y. Y., and Thorne, R. M. (2007), Dynamic evolution of energetic outer zone electrons due to wave-particle interactions during storms, *J. Geophys. Res.*, 112, A10, 2156-2202, 10.1029/2007JA012368.

Lyons, L. R., and R. M. Thorne (1972), Parasitic pitch angle diffusion of radiation belt particles by ion cyclotron waves, *J. Geophys. Res.*, 77, 5608–5616, doi:10.1029/JA077i028p05608.

Meredith, N. P., R. B. Horne, T. Kersten, B. J. Fraser, and R. S. Grew (2014), Global morphology and spectral properties of EMIC waves derived from CRRES observations, *J. Geophys. Res. Space Physics*, 119, 5328–5342, doi:10.1002/2014JA020064.

Meredith, N. P., R. M. Thorne, R. B. Horne, D. Summers, B. J. Fraser, and R. R. Anderson (2003), Statistical analysis of relativistic electron energies for cyclotron resonance with EMIC waves observed on CRRES, *J. Geophys. Res.*, *108*, 1250, doi:10.1029/2002JA009700.

Moldwin, M. B. (1997), Outer Plasmaspheric Plasma Properties: What We Know from Satellite Data, *Space Science Reviews*, 80, ISSN 0038-6308, 181-198, doi: 10.1023/A:1004921903897.

Ni, B., R. M. Thorne, Y. Y. Shprits, and J. Bortnik (2008), Resonant scattering of plasma sheet electrons by whistler-mode chorus: Contribution to diffuse auroral precipitation, *Geophys. Res. Lett.*, 35, L11106, doi:10.1029/2008GL034032.

Ni, B., et al. (2015), Resonant scattering of outer zone relativistic electrons by multiband EMIC waves and resultant electron loss time scales, *J. Geophys. Res. Space Physics*, 120, 9, 7357-7373, ISSN 2169-9402, doi:10.1002/2015JA021466

Orlova, K., and Y.Y. Shprits (2011), On the bounce-averaging of scattering rates and the calculation of bounce period, *Phys. Plasmas 18*, 092904, doi:10.1063/1.3638137.

Saikin, A. A., J.-C. Zhang, R. C. Allen, C. W. Smith, L. M. Kistler, H. E. Spence, R. B. Torbert, C. A. Kletzing, and V. K. Jordanova (2015), The occurrence and wave properties of H+-, He+-, and O+-band EMIC waves observed by the Van Allen Probes, J. Geophys. Res. Space Physics, 120, 7477–7492, doi:10.1002/2015JA021358.

Sheeley, B. W., Moldwin, M. B., Rassoul, H. K., Anderson, R. R. (2001), An empirical plasmasphere and trough density model: CRRES observations, *J. Geophys. Res. Space Physics*, 106, A11, ISSN 2156-2202, http://dx.doi.org/10.1029/2000JA000286PY

Shprits Y.Y., Subbotin D.A., Meredith N.P., Elkington S.R. (2008), Review of modeling of losses and sources of relativistic electrons in the outer radiation belt II: Local acceleration and loss, *J. Atmos. Sol. Terr. Phys.*, 70, 14, 1694-1713, ISSN 1364-6826, http://dx.doi.org/10.1016/j.jastp.2008.06.014.

Shprits, Y. Y. (2009), Potential waves for pitch-angle scattering of near-equatorially mirroring energetic electrons due to the violation of the second adiabatic invariant, Geophys. Res. Lett., 36, L12106, doi:10.1029/2009GL038322.

Shprits, Y.Y., et al. (2015), Combined convective and radial diffusive transport with pitch and energy scattering: 4D VERB results, in preparation for *Geophys. Res. Lett.*

Su, Z., F. Xiao, H. Zheng, and S. Wang (2011), CRRES observation and STEERB simulation of the 9 October 1990 electron radiation belt dropout event, *Geophys. Res. Lett.*, 38, L06106, doi:10.1029/2011GL046873.

Su, Z., H. Zhu, F. Xiao, H. Zheng, C. Shen, Y. Wang, and S. Wang (2012), Bounce-averaged advection and diffusion coefficients for monochromatic electromagnetic ion cyclotron wave: Comparison between test-particle and quasi-linear models, *J. Geophys. Res.*, 117, A09222, doi:10.1029/2012JA017917.

Su, Z., H. Zhu, F. Xiao, H. Zheng, C. Shen, Y. Wang, and S. Wang (2013), Latitudinal dependence of nonlinear interaction between electromagnetic ion cyclotron wave and radiation belt relativistic electrons, *J. Geophys. Res. Space Physics*, 118, 3188-3202, doi:10.1002/jgra.50289.

Summers, D., and R. M. Thorne (2003), Relativistic electron pitch-angle scattering by electromagnetic ion cyclotron waves during geomagnetic storms, *J. Geophys. Res.*, 108(A4), 1143, doi:10.1029/2002JA009489.

Summers, D., B. Ni, and N. P. Meredith (2007a), Timescales for radiation belt electron

acceleration and loss due to resonant wave-particle interactions: 1. Theory, *J. Geophys. Res.*, 112, A04206, doi:10.1029/2006JA011801.

Summers D., Ni B., Meredith N.P. (2007b), Timescales for radiation belt electron acceleration and loss due to resonant wave-particle interactions: 2. Evaluation for VLF chorus, ELF hiss, and electromagnetic ion cyclotron waves, *J. Geophys. Res. Space Physics*, 112, A4, ISSN 2156-2202, http://dx.doi.org/10.1029/2006JA011993

Thorne, R. M., and C. F. Kennel (1971), Relativistic electron precipitation during magnetic storm main phase, *J. Geophys. Res*., 76(19), 4446–4453, doi:10.1029/JA076i019p04446.

Ukhorskiy, A. Y., Y.Y. Shprits, B. J. Anderson, K. Takahashi, and R. M. Thorne (2010), Rapid scattering of radiation belt electrons by storm time EMIC waves, *Geophys. Res. Lett*., 37, L09101, doi:10.1029/2010GL042906.

Usanova, M.E., et al. (2014), Effect of EMIC waves on relativistic and ultrarelativistic electron populations: Ground-based and Van Allen Probes observations, *Geophys. Res. Lett., 41*, doi:10.1002/2013GL059024.

Supporting Information for

Scattering of Relativistic and Ultra-relativistic Electrons by Obliquely Propagating Electromagnetic Ion Cyclotron Waves

Bogdan Uzbekov[1], Yuri Y. Shprits[2,3,4], and Ksenia Orlova[1,2]

[1] - Skolkovo Institute of Science and Technology, Moscow, Russia.

[2] - Department of Earth, Planetary, and Space Sciences, University of California, Los Angeles, California, USA.

[3] - Department of Earth, Atmospheric and Planetary Sciences, Massachusetts Institute of Technology, Cambridge, Massachusetts, USA.

[4] - Helmholtz Centre Potsdam, GFZ German Research Centre For Geosciences.

Introduction

Material below describes quasi-linear formulation that was used in our study to calculate diffusion coefficients for oblique EMIC waves propagating in multi-ion plasma.

Full Cold Plasma Dispersion Relation

In our study we used theory of cold plasma which is defined as a collection of charged particles without any net charge that have no kinetic thermal motion on their own [*Swanson*, 2003]. Cold plasma particles can only be induced to move by self-consistent electric and magnetic fields of the wave. Cold plasma dispersion relation (CPDR) is derived in plasma physics textbooks, for example in *Stix* [1962]. CDPR in multicomponent plasma is given by the following set of expressions

$$A\mu^4 - B\mu^2 + C = 0, \tag{1}$$

where $\mu = kc/\omega$ is refractive index, and

$$A = SX^2 + P, \tag{2}$$

$$B = RLX^2 + PS(2 + X^2), \tag{3}$$

$$C = PRL(1 + X^2), \tag{4}$$

where $X = tan(\theta)$, θ is the angle between the wave normal and local geomagnetic field vector and P, R, L and S are the Stix parameters defined as

$$R = 1 - \sum_i \frac{\omega_{pi}^2}{\omega} \frac{1}{\omega + \Omega_i} \tag{5}$$

$$L = 1 - \sum_i \frac{\omega_{pi}^2}{\omega} \frac{1}{\omega - \Omega_i} \tag{6}$$

$$P = 1 - \sum_i \frac{\omega_{pi}^2}{\omega^2} \tag{7}$$

$$S = \frac{R + L}{2} \tag{8}$$

where the summations is over all the plasma species (electrons and ions), ω is the wave frequency, and ω_{pi} and Ω_i are plasma and cyclotron frequencies respectively

$$\omega_{pi}^2 = \frac{n_i e^2}{m_i \varepsilon_0} \tag{9}$$

$$\Omega_i = \frac{|q_i| B}{m_i} \tag{10}$$

Here n_i and m_i are number density and mass, respectively, of particles of species i, and B is local magnetic field value.

Substituting expressions for plasma and cyclotron frequencies (9)-(10) into expressions for the Stix parameters (5)-(8), then Stix parameters into the coefficients A, B, and C given by (2)-(4), and finally substituting resulting expressions into (1) yields cold plasma dispersion relation of the form $\mathcal{D}(k, X, \omega) = 0$. In the case of plasma consisting of electrons, hydrogen, helium, and oxygen ions expression $\mathcal{D}(k, X, \omega)$ is fourteenth order polynomial with respect to the wave frequency ω.

Computation of the Diffusion Coefficients

Bounce-averaged diffusion coefficients for oblique EMIC waves are calculated using formalism reported in [*Glauert and Horne*, 2005; *Albert*, 2005]. In this section we give summary of the equations implemented in our model.

Charged particles populating radiation belts can undergo resonant interactions with plasma waves that are present in the Earth's magnetosphere. Resonance condition is met when Doppler-shifted frequency (frequency of the wave in the electron frame of reference) of obliquely propagating circularly polarized wave is equal to multiples of electron gyrofrequency. The condition can be written as [*Stix*, 1962]

$$\omega - k_{\parallel} v_{\parallel} = \frac{n \Omega_e}{\gamma} \tag{11}$$

where $k_{\parallel}$ and $v_{\parallel}$ are parallel components (with respect to local geomagnetic field vector) of wave normal and electron velocity vectors, $n = 0, \pm 1, \pm 2, \pm 3, \ldots$ is called resonance harmonic number, and γ is relativistic Lorentz factor.

Thus, waves satisfying resonance condition (11) and plasma dispersion relation $\mathcal{D}(k, X, \omega) = 0$ can resonantly interact with RB electrons causing diffusion in adiabatic invariants.

Pitch angle and momentum local diffusion coefficients are defined as

$$D_{\alpha\alpha} = \frac{1}{2} \langle \frac{(\Delta\alpha)^2}{\Delta t} \rangle \tag{12}$$

$$D_{\alpha p} = \frac{1}{2p}\langle\frac{\Delta\alpha\Delta p}{\Delta t}\rangle \tag{13}$$

$$D_{pp} = \frac{1}{2p^2}\langle\frac{(\Delta p)^2}{\Delta t}\rangle \tag{14}$$

where $\langle(\Delta\alpha)^2/\Delta t\rangle$ denotes the expected value of change of $(\Delta\alpha)^2$ per unit time Δt of for a particle with pitch angle α, and term $\langle\Delta\alpha\Delta p/\Delta t\rangle$ has similar definition.

In order to calculate diffusion coefficients we assume that wave spectral power density $B^2(\omega)$ is distributed normally following *Lyons* [1974]

$$B^2(\omega) = \begin{cases} A^2 exp\left(-\left(\frac{\omega-\omega_m}{\delta\omega}\right)^2\right), & \omega_{lc} \le \omega \le \omega_{uc} \\ 0, & otherwise \end{cases} \tag{15}$$

where B^2 is measured in T^2/Hz, ω_m and $\delta\omega$ are distribution maximum and bandwidth respectively, ω_{lc} and ω_{uc} are lower and upper cut-off frequencies, and A is a normalization factor given by

$$A^2 = \frac{|B_w|^2}{\delta\omega}\frac{2}{\sqrt{\pi}}\left[erf\left(\frac{\omega_m-\omega_{lc}}{\delta\omega}\right) + erf\left(\frac{\omega_{uc}-\omega_m}{\delta\omega}\right)\right]^{-1} \tag{16}$$

where B_w is the wave amplitude measured in Tesla.

The distribution of the tangent of wave normal angle θ is also assumed to be Gaussian:

$$g(X) = \begin{cases} exp\left(-\left(\frac{X-X_m}{X_w}\right)^2\right), & X_{min} \le X \le X_{max} \\ 0, & otherwise \end{cases} \tag{17}$$

where X_w is the angular distribution bandwidth, X_m is the peak, and X_{min} and X_{max} are the cut-off values.

Given these definitions, local diffusion coefficients can be written as

$$D_{\alpha\alpha} = \frac{1}{p^2}\sum_{n=n_l}^{n=n_h}\int_{X_{min}}^{X_{max}} X dX\, D_{\alpha\alpha}^{nX} \tag{18}$$

$$D_{\alpha p} = \frac{1}{p^2}\sum_{n=n_l}^{n=n_h}\int_{X_{min}}^{X_{max}} X dX\, D_{\alpha p}^{nX} \tag{19}$$

$$D_{pp} = \frac{1}{p^2}\sum_{n=n_l}^{n=n_h}\int_{X_{min}}^{X_{max}} X dX\, D_{pp}^{nX} \tag{20}$$

where the summation is over the resonant harmonics and

$$D_{\alpha\alpha}^{nX} =$$

$$= \sum_i \frac{q_e^2 \omega_i^2}{4\pi(1+X^2)N(\omega_i)} \left[\frac{n\Omega_e/\gamma\omega_i - sin^2\alpha}{cos\alpha}\right]^2 B^2(\omega_i) g(X) \frac{\left|\Phi_{n,k}\right|^2}{\left|\vartheta_\parallel - \frac{\partial\omega}{\partial k_\parallel}\Big|_{\mathcal{D}=0}\right|}\Bigg|_{k_{\parallel i}} \tag{21}$$

$$D_{\alpha p}^{nX} = D_{\alpha\alpha}^{nX}\left[\frac{\sin(\alpha)\cos(\alpha)}{n\Omega_e/\gamma\omega_i - sin^2\alpha}\right] \tag{22}$$

$$D_{pp}^{nX} = D_{\alpha\alpha}^{nX}\left[\frac{\sin(\alpha)\cos(\alpha)}{n\Omega_e/\gamma\omega_i - sin^2\alpha}\right]^2 \tag{23}$$

and quantities $D_{\alpha\alpha}^{nX}$, $D_{\alpha p}^{nX}$ and D_{pp}^{nX} are evaluated at the resonant parallel wave number and resonant frequency, $k_{\parallel i}$ and ω_i respectively, that are found by solving a set of resonance condition (11) and of plasma dispersion relation equations:

$$\begin{cases} \omega - k_\parallel v_\parallel = \dfrac{n\Omega_e}{\gamma} \\ \mathcal{D}(k,\omega,X) = 0 \end{cases} \tag{24}$$

It is important to notice that derivative $\partial\omega/\partial k_\parallel\big|_{\mathcal{D}=0}$ in (21) is calculated along the dispersion relation line $\mathcal{D}(k,X,\omega) = 0$.

Functions $\left|\Phi_{n,k}\right|^2$ and $N(\omega)$ are given by

$$\left|\Phi_{n,k}\right|^2 =$$
$$= \left[\left(\left(\frac{\mu^2-L}{\mu^2-S}\right)J_{n+1} + \left(\frac{\mu^2-R}{\mu^2-S}\right)J_{n-1}\right.\right.$$
$$\left.\left. + tan^{-1}(\alpha)sin(\psi)cos(\psi)J_n\right)\left(\frac{\mu^2 sin^2(\psi) - P}{2\mu^2}\right)\right]^2 \left[\left(\frac{R-L}{2(\mu^2-S)}\right)^2 \left(\frac{P-\mu^2 sin^2(\psi}{\mu^2}\right.\right.$$
$$\left.\left. + \left(\frac{Pcos(\psi)}{\mu^2}\right)^2\right]^{-1} \tag{25}$$

$$N(\omega) = \frac{1}{2\pi^2}\int_{X_{min}}^{X_{max}} \frac{g(X)k^2}{(1+X^2)^{1/2}} \frac{\partial\mathcal{D}}{\partial\omega}\left[\frac{\partial\mathcal{D}}{\partial k}\right]^{-1} XdX \tag{26}$$

where R, L, P and S are the Stix parameters defined above, μ is the refractive index, and J_n is the n^{th} order Bessel function with argument $k_\perp\vartheta_\perp/m_e\Omega_e$ (n being resonant harmonic).

Finally, we average the local diffusion coefficients over the bounce motion. Bounce averaging is obtained by integrating between the mirror points along the bounce motion path and weighting each element of the path by the time that particle spends at that increment.

It can be shown that bounce averaged values for $D_{\alpha\alpha}$, $D_{\alpha p}$, and D_{pp} are given by

$$\langle D_{\alpha_{eq}\alpha_{eq}} \rangle = \frac{1}{\tau_B} \int_0^{\tau_B} D_{\alpha\alpha} \left(\frac{\partial \alpha_{eq}}{\partial \alpha} \right)^2 dt \tag{27}$$

$$\langle D_{\alpha_{eq}p} \rangle = \frac{1}{\tau_B} \int_0^{\tau_B} D_{\alpha p} \left(\frac{\partial \alpha_{eq}}{\partial \alpha} \right) dt \tag{28}$$

$$\langle D_{pp} \rangle = \frac{1}{\tau_B} \int_0^{\tau_B} D_{pp}\, dt \tag{29}$$

where τ_B is particle's bounce period and α_{eq} is particle's equatorial pitch angle that can be obtained from the local pitch angle using conservation of the first adiabatic invariant (magnetic moment). Changing integration variable to magnetic latitude and using dipole geomagnetic field model yields

$$\langle D_{\alpha_{eq}\alpha_{eq}} \rangle = \frac{1}{T} \int_0^{\lambda_m} D_{\alpha\alpha} \frac{cos\alpha}{cos^2\alpha_{eq}} cos^7\lambda d\lambda \tag{30}$$

$$\langle D_{\alpha_{eq}p} \rangle = \frac{1}{T} \int_0^{\lambda_m} D_{\alpha p} \frac{cos^4\lambda(1+3sin^2\lambda)^{1/4} d\lambda}{cos\alpha} \tag{31}$$

$$\langle D_{pp} \rangle = \frac{1}{T} \int_0^{\lambda_m} D_{pp} \frac{cos\lambda(1+3sin^3\lambda)^{1/2} d\lambda}{cos\alpha} \tag{32}$$

where λ_m is the mirror latitude, and $T(\alpha_{eq})$ gives variation of τ_B with the equatorial pitch angle

$$T(\alpha_{eq}) = 1.38 - 0.32sin(\alpha_{eq}) \tag{33}$$

Mirror latitude is found by solving

$$x^6 + 3x \cdot sin^4(\alpha_{eq}) - 4sin^4(\alpha_{eq}) = 0 \tag{34}$$

where $x = cos^2(\lambda_m)$.

References

Albert, J. M. (2005), Evaluation of quasi-linear diffusion coefficients for whistler mode waves in a plasma with arbitrary density ratio, J. Geophys. Res., 110, A03218, doi:10.1029/2004JA010844.

Glauert, S. A., and R. B. Horne (2005), Calculation of pitch angle and energy diffusion coefficients with the PADIE code, *J. Geophys. Res.*, 110, A04206, doi:10.1029/2004JA010851.

Lawrence R. Lyons (1974). Pitch angle and energy diffusion coefficients from resonant interactions with ion–cyclotron and whistler waves. Journal of Plasma Physics, 12, pp 417-432 doi:10.1017/S002237780002537X

Stix, T. H., The Theory of Plasma Waves, McGraw-Hill, New York, 1962.

Swanson D. G., Plasma Waves, 2nd Edition, Taylor and Francis, 2003.

Highlights for

Scattering of Relativistic and Ultra-relativistic Electrons by Obliquely Propagating Electromagnetic Ion Cyclotron Waves

Bogdan Uzbekov[1], Yuri Y. Shprits[2,3,4], and Ksenia Orlova[1,2]

[1] - Skolkovo Institute of Science and Technology, Moscow, Russia.

[2] - Department of Earth, Planetary, and Space Sciences, University of California, Los Angeles, California, USA.

[3] - Department of Earth, Atmospheric and Planetary Sciences, Massachusetts Institute of Technology, Cambridge, Massachusetts, USA.

[4] - Helmholtz Centre Potsdam, GFZ German Research Centre For Geosciences.

1. Presented method can be applied to EMIC waves or any other wave modes;
2. First order resonance dominates the scattering of relativistic electrons up to multi-MeV energies;
3. Ion composition is a crucial parameter for quantifying scattering rates.

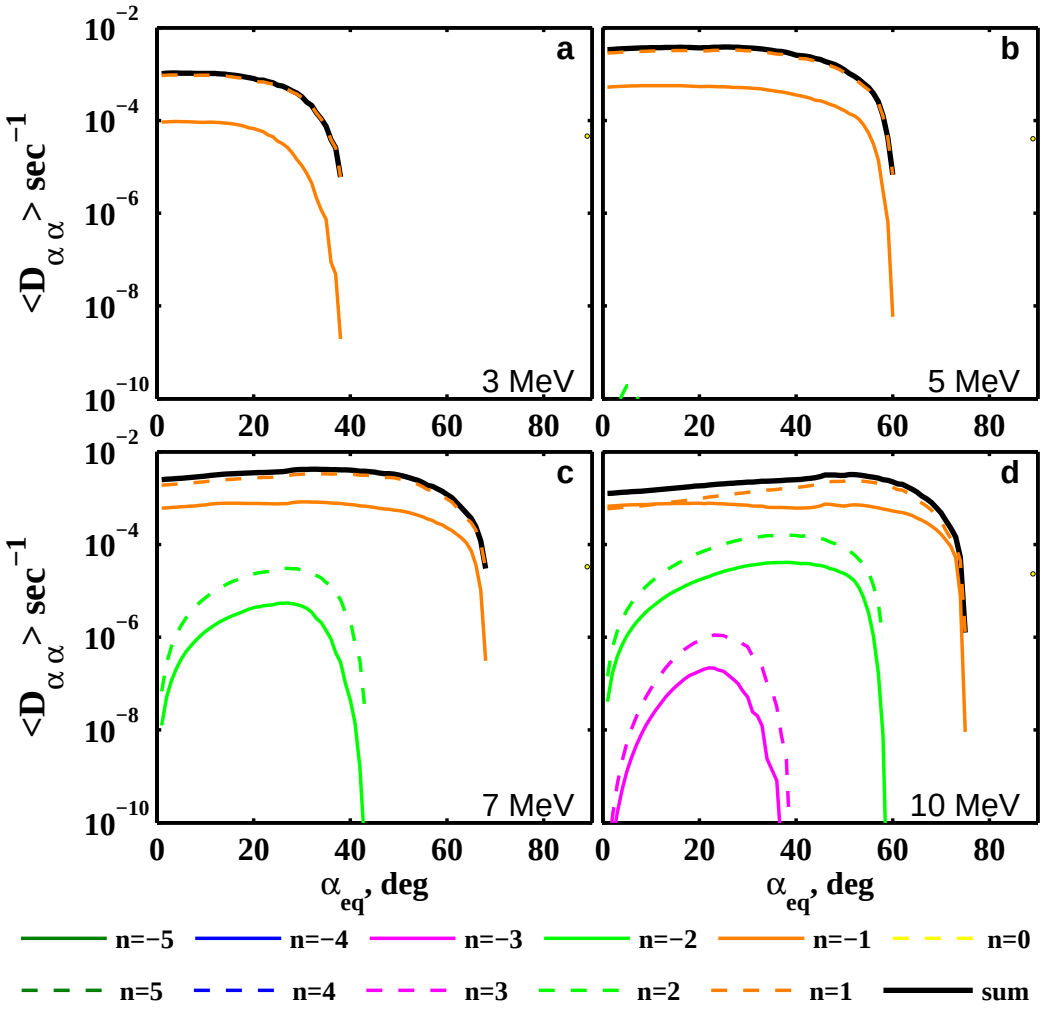
a
b
c
d
3 MeV
5 MeV
7 MeV
10 MeV
$<D_{\alpha\alpha}> sec^{-1}$
α_{eq}, deg
10^{-2}
10^{-4}
10^{-6}
10^{-8}
10^{-10}
0
20
40
60
80
n=−5
n=−4
n=−3
n=−2
n=−1
n=0
n=5
n=4
n=3
n=2
n=1
sum

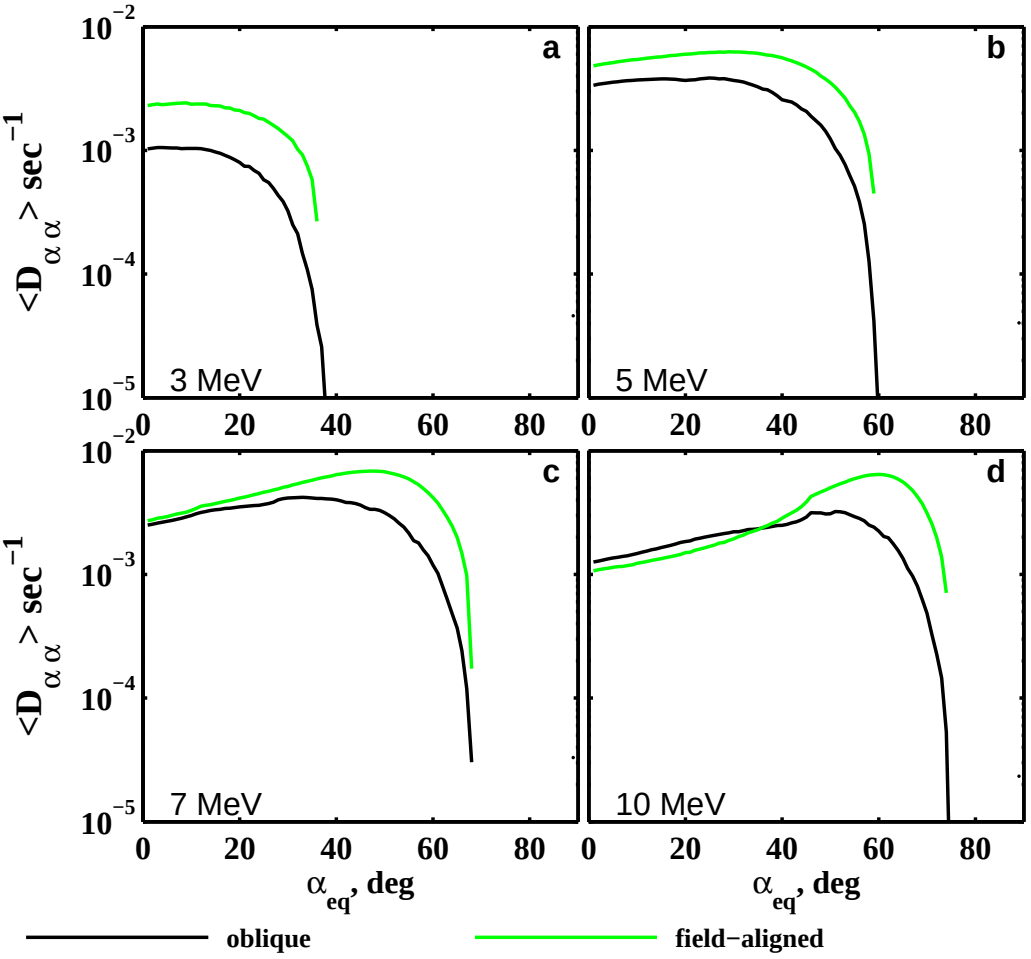
a
b
c
d
3 MeV
5 MeV
7 MeV
10 MeV
10^{-2}
10^{-3}
10^{-4}
10^{-5}
0
20
40
60
80
$<D_{\alpha\alpha}> sec^{-1}$
α_{eq}, deg
oblique
field−aligned

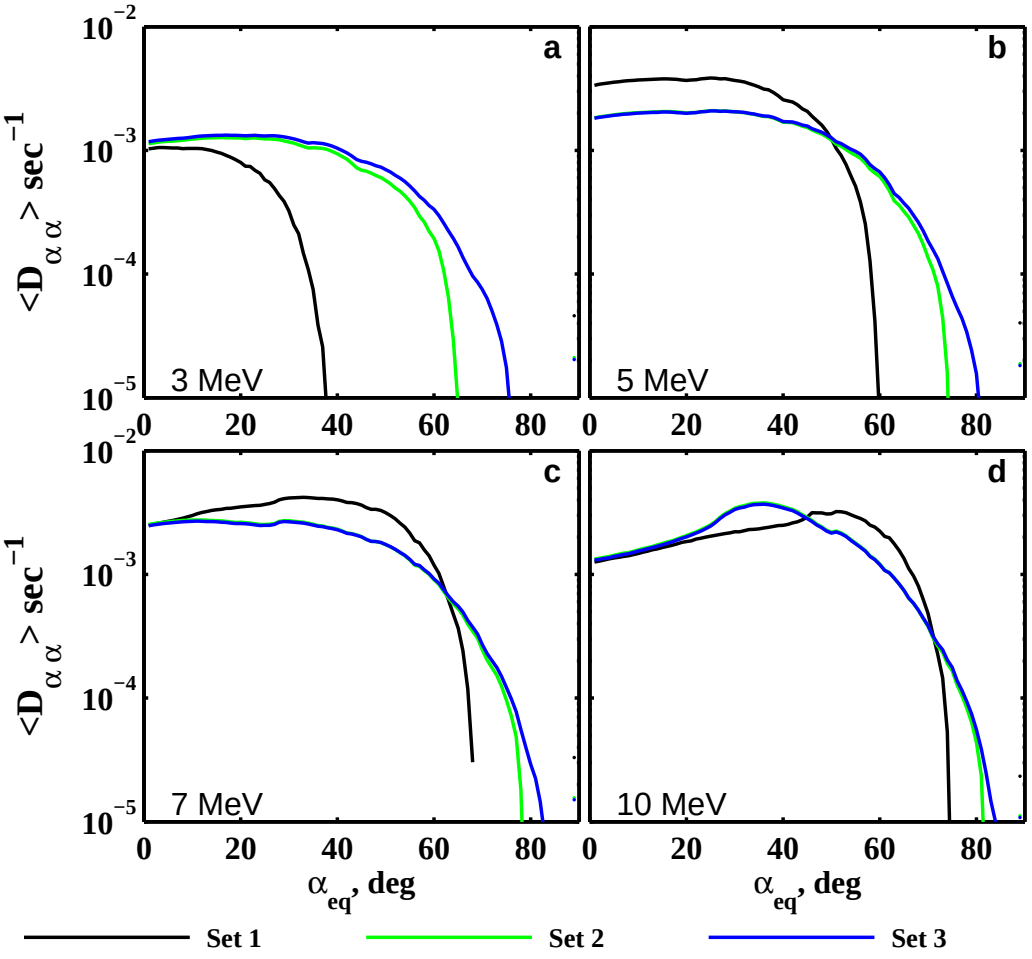
a
b
c
d
3 MeV
5 MeV
7 MeV
10 MeV
10^{-2}
10^{-3}
10^{-4}
10^{-5}
0
20
40
60
80
$<D_{\alpha\alpha}>$ sec^{-1}
α_{eq}, deg
Set 1
Set 2
Set 3

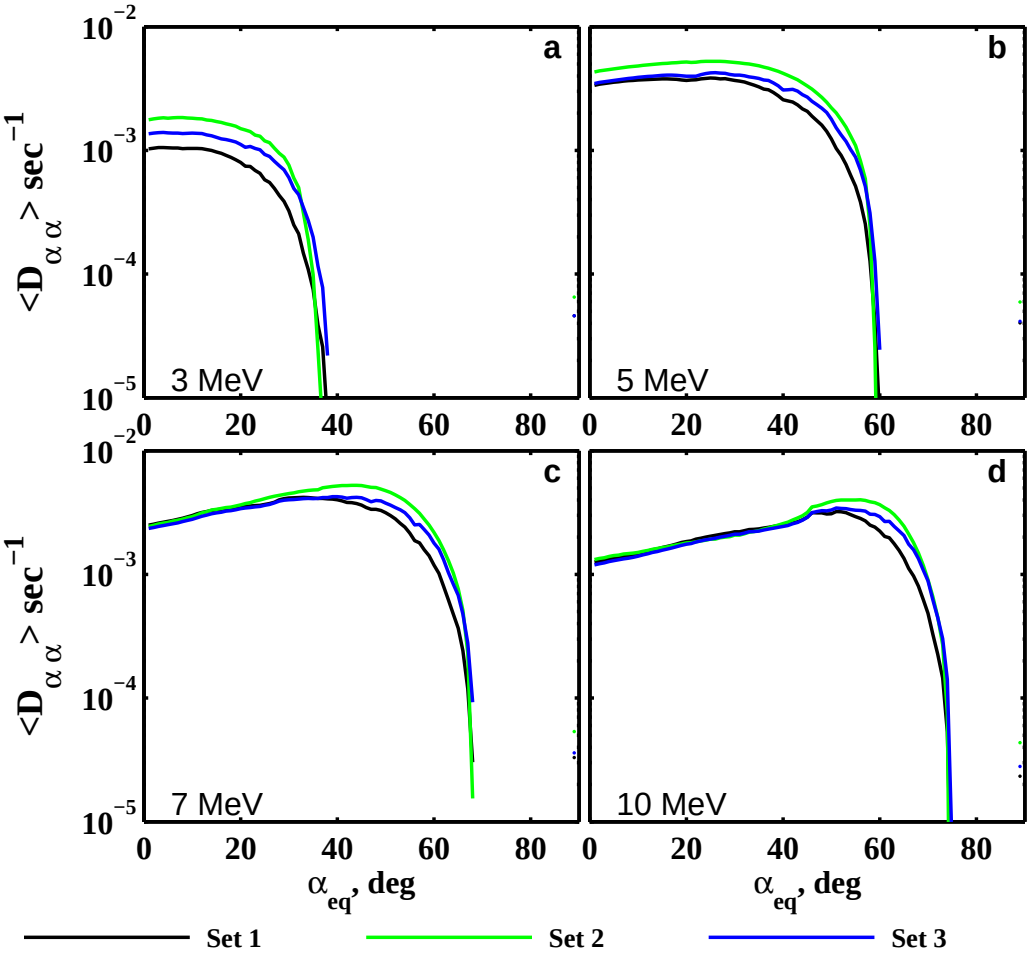
a
b
c
d
3 MeV
5 MeV
7 MeV
10 MeV
10^{-2}
10^{-3}
10^{-4}
10^{-5}
0
20
40
60
80
$<D_{\alpha\alpha}> sec^{-1}$
α_{eq}, deg
Set 1
Set 2
Set 3

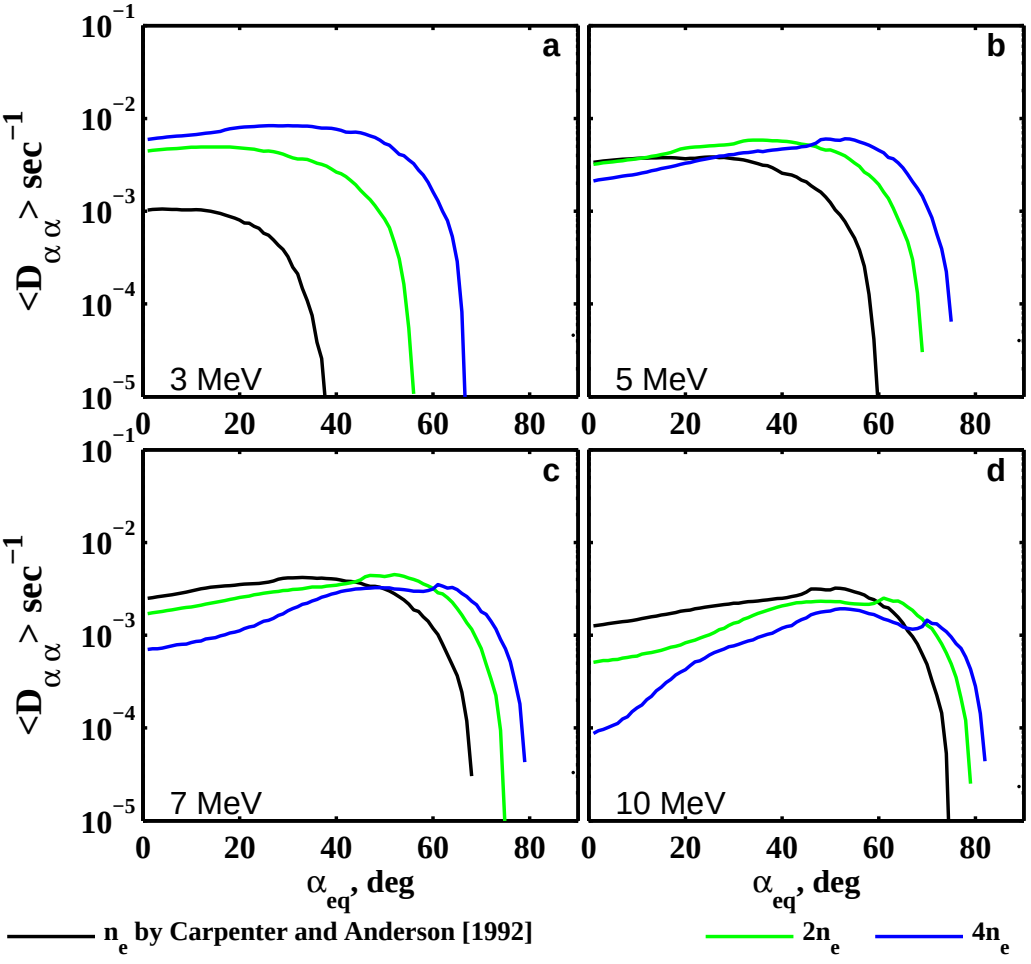
a
b
c
d
3 MeV
5 MeV
7 MeV
10 MeV
10^{-1}
10^{-2}
10^{-3}
10^{-4}
10^{-5}
0
20
40
60
80
$<D_{\alpha\alpha}> sec^{-1}$
α_{eq}, deg
n_e by Carpenter and Anderson [1992]
$2n_e$
$4n_e$

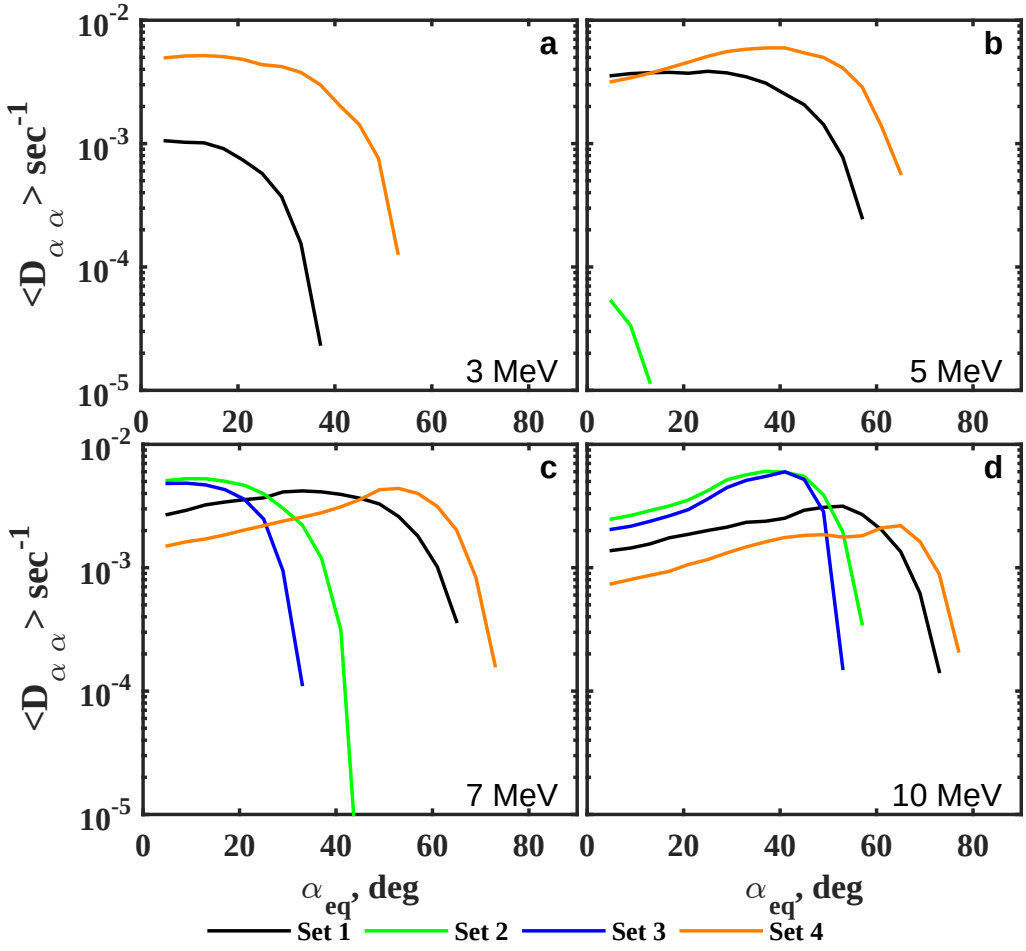
a
b
c
d
3 MeV
5 MeV
7 MeV
10 MeV
10^{-2}
10^{-3}
10^{-4}
10^{-5}
0
20
40
60
80
$<D_{\alpha\alpha}> sec^{-1}$
α_{eq}, deg
Set 1
Set 2
Set 3
Set 4